

Structural evolution from iron sulfide nanoparticle to pyrite

Yoshinari Sano,* Atsushi Kyono and Sota Takagi

University of Tsukuba, 1-1-1 Tennodai, Tsukuba, 305-8572 Japan

1 Introduction

Iron sulfide minerals play a major role in controlling the redox chemistry in anaerobic marine and lake sediments. Sulfide ion (S^{2-}) is reduced from sulfate ion (SO_4^{2-}) by the metabolic activity of sulfate-reducing bacteria (SRB), but it is re-oxidized to sulfur (S^0) and further oxidized to sulfate ion (SO_4^{2-}) by the sulfur bacteria (SB) in the sedimentary environments. This biological sulfur cycle is one of the most important elemental cycles at the Earth's surface. Iron sulfide (FeS) nanoparticles are initially formed by reaction between the ferrous iron (Fe^{2+}) and the sulfide ion (S^{2-}) (Berner 1967). The FeS nanoparticle, which shows the X-ray amorphous nature, consists of disordered arrangement of FeS_4 tetrahedral sheets (Wolthers et al., 2003; Ohfuji and Rickard, 2006; Csákberényi-Malasics et al., 2012). Under the anoxic aqueous conditions, it is gradually evolved to more stable iron sulfide minerals. By grain growth, the FeS nanoparticle transforms to mackinawite (FeS), consisting of the FeS_4 tetrahedral sheets (Jeong et al., 2008; Csákberényi-Malasics et al., 2012). By the oxidation of ferrous (Fe^{2+}) to ferric (Fe^{3+}) iron, the mackinawite further transforms to the thiospinel iron sulfide mineral, greigite (Fe_3S_4) (Schoonen and Barnes, 1991; Jeong et al., 2008; Csákberényi-Malasics et al., 2012). By supply of sulfur (S^0), the FeS_4 tetrahedral coordination changes into FeS_6 octahedral coordination in the structure, which leads to pyrite with the perfect long-range atomic order (Schoonen and Barnes, 1991). Therefore, the pyrite is the most abundant sulfide mineral at the Earth's surface (Rickard, 2012).

Despite the numerous studies and the importance of pyrite formation in the biological sulfur cycle, the transformation mechanism from the FeS nanoparticle to pyrite has not been fully understood.

In the present study, hydrothermal experiments and X-ray crystal structural analysis were performed to clarify the phase transformation and structural change mechanism from the FeS nanoparticle to pyrite.

2 Experiment

In the study, deoxygenated water was applied in all experiments due to the high reactivity of the FeS nanoparticle toward oxygen. The deoxygenated water was prepared by bubbling N_2 gas to distilled water. First, the FeS nanoparticle suspension was obtained by mixing 10 mL of 0.2 M $(NH_4)_2Fe(SO_4)_2 \cdot 6H_2O$ aqueous solution with 10 mL of 0.4 M $Na_2S \cdot 9H_2O$ aqueous solution in a glove box with an inert N_2 atmosphere. The obtained black suspension was then filtered through a 0.1 μm membrane filter (Merck Millipore Ltd) and blow-dried with N_2 gas. Subsequently, it was kept in a vacuum desiccator until used. In order to induce the phase transformation from the FeS nanoparticle to pyrite, the FeS nanoparticle suspension was

transferred into the Teflon container with 77 mg sulfur powder. The hydrothermal experiments were performed at 120°C for 2, 4, 6, 8, 12, 16, 20, and 24 hours. After heating for various periods, the resulting suspensions were filtered in the same way and stored in the vacuum desiccator.

Synchrotron powder X-ray diffraction (XRD) measurements were conducted at BL-8B of PF in KEK. In order to avoid any oxidation of the samples, they were inserted into the glass capillary ($\phi = 0.7$ mm). The wavelength of X-ray was 0.6868 (5) Å. The exposure time was set to 30 minutes. The obtained XRD data were analyzed with PDIndexer software (Seto et al., 2010).

Fe K-edge X-ray absorption fine structure (XAFS) measurements were performed at BL-9C of PF in KEK. The XAFS station was equipped with Si(111) double crystal monochromator. 4 mg of the sample was diluted with 150 mg of BN powder and pressed into pellets with a diameter of 10 mm under N_2 atmosphere. Ionization chambers filled with 100% N_2 and 15% Ar in N_2 were used to measure the incident and transmitted X-ray intensities, respectively. All spectra were collected in transmission mode at room temperature. Energy measurement range was set from 6606.2 to 8211.3 eV. Energy calibration was carried out using spectrum of Fe foil. The obtained XAFS spectra were corrected and normalized using the Athena software (Ravel and Newville, 2005). The EXAFS spectra were imported into Artemis software (Ravel and Newville, 2005), and fitted to theoretical models of mackinawite and pyrite using Atoms (Ravel, 2001) and FEFF6 code (Rehr et al 1991).

3 Results and Discussion

Figure 1 shows the variation of synchrotron XRD pattern. At 120°C the FeS nanoparticle was changed to pyrite as a function of heating time. The FeS nanoparticle, unheated black suspension, showed characteristic broad XRD maxima. The fact that the XRD pattern was nearly the same to that of mackinawite suggests that the FeS nanoparticle basically consists of mackinawite-like structure. This result is approximately consistent with the previous TEM observation (Ohfuji and Rickard, 2006). After heating for 8 h, the weak XRD peaks from pyrite and greigite appeared. After further heating for 16 h, the XRD peaks from mackinawite completely disappeared. Finally, only pyrite and greigite were observed. Therefore, most of the FeS nanoparticle directly changed into the more stable pyrite by the reaction with sulfur ($FeS + S \rightarrow FeS_2$), but a small amount of the FeS nanoparticle transformed to greigite by oxidation of ferrous (Fe^{2+}) to ferric iron (Fe^{3+}). The previous studies (Rickard and Morse, 2005; Jeong et al., 2008; White et al., 2015) also indicated that greigite was formed by oxidation of FeS nanoparticle in water under anoxic solution condition ($4FeS + 2H_2O \rightarrow Fe_3S_4 +$

$\text{Fe}(\text{OH})_2\text{aq} + \text{H}_2$). It can be therefore considered that the anoxic water acts as oxidant which oxidizes ferrous iron

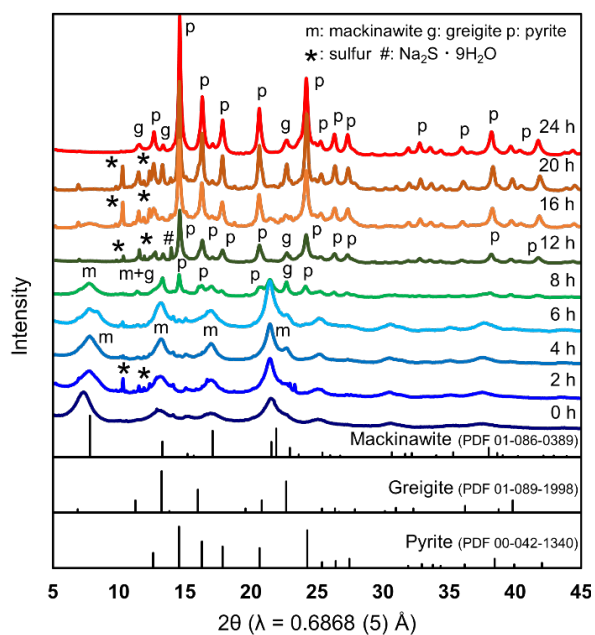


Fig. 1. Variation of XRD pattern as a function of heating time (Fe^{2+}) to ferric iron (Fe^{3+}).

Figure 2 shows the variation of radial structure functions (RSF) and fitting results with mackinawite and pyrite structures. The RSF pattern of FeS nanoparticle, unheated black suspension, shows only first shell, which indicates that there are only four S atoms around the Fe atom. This is, the FeS nanoparticle is solely composed of FeS_4 tetrahedra without any long-range atomic order.

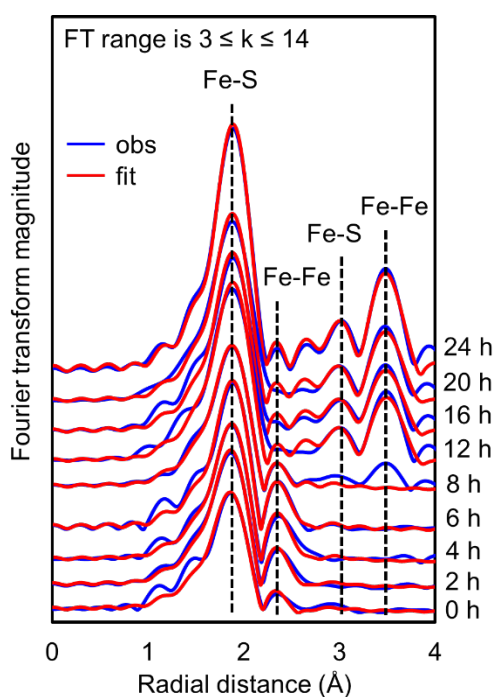


Fig. 2. Radial structure functions (RSF)

As it can be seen in Figure 2, the RSF patterns from 2 to 6 h apparently consist of two shells. The first shell corresponds to the four S atoms bonded to the central Fe atom, whereas the second shell is ascribed to the Fe atoms adjacent to the central Fe atom. This appearance of the second shell implies that a long-range order of FeS_4 tetrahedra is established by heating. Csákerényi-Malasics et al. (2012) documented that the crystal growth from FeS nanoparticle to mackinawite proceeded under anoxic hydrothermal condition at 120°C. Our result is therefore in good agreement with the previous study (Csákerényi-Malasics et al., 2012). The RSF patterns from 12 to 24 h were well fitted with pyrite structure, but the RSF of 8 h showed an intermediate profile between FeS nanoparticle and pyrite. The FeS nanoparticle transformed gradually to pyrite by the reaction with sulfur during heating from 8 to 12 h. The result obtained by RSF patterns seems to be fully compatible with the XRD measurements.

Figure 3 shows the changes of Fe-S bond distance and coordination number (CN). In spite of heating time, the Fe-S bond distance of about 2.26 Å remained unchanged. Lennie et al. (1995) reported that the Fe-S bond distance in mackinawite was 2.256 Å. On the other hand, the corresponding bond distance in greigite was 2.147 Å (Skinner et al., 1964). Therefore, the Fe-S bond distance in the FeS nanoparticle is entirely consistent with that in mackinawite. Fe in FeS_4 tetrahedra has a formal valence of +2 in mackinawite, but that in greigite gives an average valence of +2.5 by the electron hopping. Since the Fe in FeS nanoparticle is in the similar tetrahedral coordination to mackinawite, it also has a formal valence of +2.

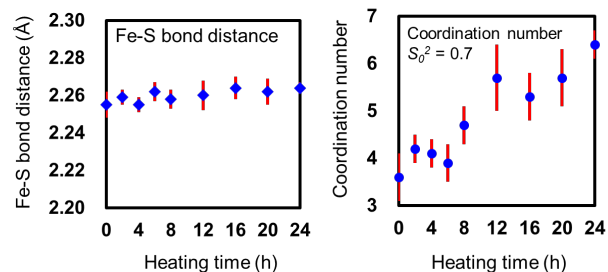


Fig. 3. The changes of Fe-S bond distance and coordination number (CN)

During heating for 8 h the CN of about 4 was maintained constant within the experimental error, but it was increased to 6 after heating for 12 h. This must be ascribed to the coordination change from FeS_4 tetrahedron to FeS_6 octahedron. That is, the FeS nanoparticle entirely transformed to pyrite. Since the Fe-S bond distance in pyrite is 2.264 Å (Willeke et al., 1992), the evidence that the Fe-S bond distance remained unchanged throughout the heating experiment supports the direct phase transformation from the FeS nanoparticle to pyrite. In the previous hydrothermal in-situ ED-XRD study, Hunger and Benning, (2007) reported that at temperatures above 125°C mackinawite transformed to pyrite through greigite as an intermediate phase. In the present study, however, the peaks corresponding to greigite was never detected in the PSF patterns because no characteristic short and long Fe-S

bond distances in greigite (2.147 and 2.464 Å) were clearly detected. Therefore, the directly phase transformation from the FeS nanoparticle to pyrite could preferentially occur at temperatures below 120 °C.

Figure 4 shows the local atomic structure changes from the FeS nanoparticle to pyrite. Local atomic structure of the unheated FeS nanoparticle consists of the FeS₄ tetrahedron without any long-range atomic order, which exhibits the X-ray amorphous nature. After heating for 6 h, the FeS₄ tetrahedra started to connect linearly each other along one direction. The Fe-Fe atomic distance of 2.69(1) Å in the FeS nanoparticle is however still larger than that in mackinawite (Fe-Fe = 2.598 Å; Lennie et al., 1995). This result suggests that the crystal structure of the FeS nanoparticle is slightly different from that of mackinawite previously reported. The small angle X-ray scattering study (Wolthers et al., 2003) and TEM observation (Ohfuji and Rickard, 2006; Csákbereányi-Malasics et al., 2012) showed that the FeS₄ tetrahedral sheets in FeS nanoparticle are more or less curved. Therefore, the larger Fe-Fe atomic distance in the FeS nanoparticle could result from distortion in the FeS₄ tetrahedral sheets. After heating for 12 h, the S-S bonds formation and coordination number change of Fe occur (Figs. 2 and 3), which indicates the formation of pyrite.

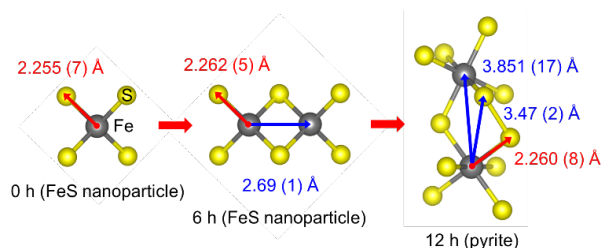


Fig. 4: The local atomic structure changes

4 Conclusions

In the study, the phase transformation and structural change mechanism from FeS nanoparticle to pyrite were investigated by using hydrothermal experiments, synchrotron XRD measurements, and EXAFS analysis. The result of synchrotron XRD analysis showed that the most of FeS nanoparticle directly transformed to pyrite by the reaction with sulfur, but a small amount of FeS nanoparticle was oxidized and transformed to greigite. The local atomic structure analysis revealed that the FeS nanoparticle consists of distorted FeS₄ tetrahedral sheets. By heating for 12 h, the FeS₄ tetrahedra directly change into the FeS₆ octahedra, which results in the formation of pyrite. These results provide fundamental data of the mineral formation and structural behaviours of the FeS nanoparticle and pyrite in anaerobic aqueous environments.

Acknowledgement

We sincerely thank Y. Niwa and H. Nitani for their kind assistance and technical advice.

References

- [1] Berner, R. A. (1967) Thermodynamic stability of sedimentary iron sulfides. *American Journal of Science*, 265, 773-785.
- [2] Schoonen, M. A. A. and Barnes, H. L. (1991) Mechanisms of pyrite and marcasite formation from solution. *Geochimica et Cosmochimica Acta*, 55, 3491-3504.
- [3] Wolthers, M., Van der Gaast, S., Rickard, D. (2003) The structure of disordered mackinawite. *American Mineralogist* 88, 2007–2015.
- [4] Ohfuji H. and Rickard D. (2006) High resolution transmission electron microscopic study of synthetic nanocrystalline mackinawite. *Earth and Planetary Science Letters*, 241, 227-233.
- [5] Hunger S. Benning L.G. (2007) Greigite: a true intermediate on the polysulfide pathway to pyrite. *Geochemical Transactions* 8 (1), 1–20.
- [6] Jeong H.Y. Lee J.H. Hayes K.F. (2008) Characterization of synthetic nanocrystalline mackinawite: crystal structure, particle size, and specific surface area. *Geochimica et Cosmochimica Acta* 72, 493–505.
- [7] Csakberenyi-Malasics D. Rodriguez-Blanco J. Kias V. Recnik A. Benning L. G. Posfai M. (2012) Structural properties and transformation precipitated FeS. *Chemical Geology*, 294-295, 249-258.
- [8] White L.M. Bhartia R. Stucky G.D. Kanik I. and Russell M.J. (2015) Mackinawite and greigite in ancient alkaline hydrothermal chimneys: identifying potential key catalysts for emergent life. *Earth and Planetary Science Letters*, 430:105–114.

* sano@geol.tsukuba.ac.jp